

Received 27 November 2014; revised 14 February 2015; accepted 10 March 2015. Date of publication 10 April 2015;
date of current version 29 April 2015.

Digital Object Identifier 10.1109/JTEHM.2015.2421901

Automatic Real-Time Embedded QRS Complex Detection for a Novel Patch-Type Electrocardiogram Recorder

DORTHE B. SAADI^{1,2}, GEORGE TANEV², MORTEN FLINTRUP², ARMIN OSMANAGIC³,
KENNETH EGSTRUP³, KARSTEN HOPPE², POUL JENNUM⁴, JØRGEN L. JEPPESEN⁵,
HELLE K. IVERSEN⁶, AND HELGE B. D. SORENSEN¹, (Member, IEEE)

¹Department of Electrical Engineering, Technical University of Denmark, Kongens Lyngby 2800, Denmark

²DELTA Danish Electronics, Light and Acoustics, Hørsholm 2970, Denmark

³Department of Medical Research, Svendborg Hospital, Odense University Hospital, Svendborg 5700, Denmark

⁴Danish Center for Sleep Medicine, Department of Clinical Neurophysiology, Glostrup Hospital, University of Copenhagen, Glostrup 2600, Denmark

⁵Department of Medicine, Glostrup Hospital, Glostrup 2600, Denmark

⁶Department of Neurology, Glostrup Hospital, Glostrup 2600, Denmark

CORRESPONDING AUTHOR: D. B. SAADI (dorthe_bodholt@hotmail.com)

This work was supported by DELTA Performance Contract 2010-2012: Intelligent Welfare Technologies and Single Use Devices,
Supported by the Danish Council for Technology and Innovation.

ABSTRACT Cardiovascular diseases are projected to remain the single leading cause of death globally. Timely diagnosis and treatment of these diseases are crucial to prevent death and dangerous complications. One of the important tools in early diagnosis of arrhythmias is analysis of electrocardiograms (ECGs) obtained from ambulatory long-term recordings. The design of novel patch-type ECG recorders has increased the accessibility of these long-term recordings. In many applications, it is furthermore an advantage for these devices that the recorded ECGs can be analyzed automatically in real time. The purpose of this study was therefore to design a novel algorithm for automatic heart beat detection, and embed the algorithm in the CE marked ePatch heart monitor. The algorithm is based on a novel cascade of computationally efficient filters, optimized adaptive thresholding, and a refined search back mechanism. The design and optimization of the algorithm was performed on two different databases: The MIT-BIH arrhythmia database ($Se = 99.90\%$, $P^+ = 99.87\%$) and a private ePatch training database ($Se = 99.88\%$, $P^+ = 99.37\%$). The offline validation was conducted on the European ST-T database ($Se = 99.84\%$, $P^+ = 99.71\%$). Finally, a double-blinded validation of the embedded algorithm was conducted on a private ePatch validation database ($Se = 99.91\%$, $P^+ = 99.79\%$). The algorithm was thus validated with high clinical performance on more than 300 ECG records from 189 different subjects with a high number of different abnormal beat morphologies. This demonstrates the strengths of the algorithm, and the potential for this embedded algorithm to improve the possibilities of early diagnosis and treatment of cardiovascular diseases.

INDEX TERMS Automatic QRS complex detection, embedded ECG analysis, ePatch ECG recorder, patch type ECG recorder, real-time ECG analysis.

I. INTRODUCTION

Cardiovascular diseases (CVDs) are projected to remain the single leading cause of death globally. According to the World Health Organization (WHO), as much as 30% of all deaths in 2008 were caused by CVDs [1]. These diseases are also a major economic burden to the healthcare facilities. One of the important diagnostic tools for timely detection and diagnosis of heart arrhythmias is ambulatory

electrocardiography (ECG) recordings. The standard equipment for this has for many years been the Holter recorder. However, the traditional Holter system possesses a number of issues that prevents prolonged monitoring. To overcome this, a number of patch type ECG recorders have recently reached the market [2], [3]. We have chosen to apply the ePatch ECG recorder designed by DELTA [3]. The ePatch is illustrated in Fig. 1 together with a short

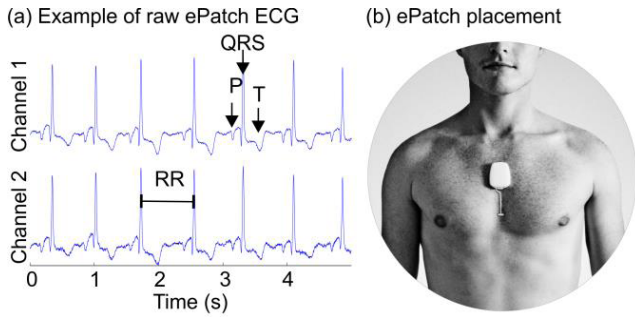


FIGURE 1. (a) Example of two channel raw ePatch ECG. The most relevant ECG fiducial points are indicated. (b) Illustration of the ePatch ECG recorder correctly placed on the chest. Each recording contains two ECG channels sampled at 512 Hz with a resolution of 12 bits. In compliance with [18], the ePatch sensor has an analog BP filter between 0.67 Hz and 40 Hz. Modified from [3].

two-channel ECG snippet. These type of recorders provide the possibility of an extended monitoring period, and studies have shown how this can ensure detection of more significant arrhythmias and lead to a definitive diagnosis for more patients [2], [4], [5]. Furthermore, some patches possess the possibility of wireless data transmission and automatic real-time embedded processing of the recorded signals. This might allow real-time transmission of e.g. arrhythmia events to a central monitoring station. The first step in this analysis is automatic detection of QRS complexes. This field has been investigated in the literature for at least 30 years [6]. Generally, the automatic QRS complex detection can be divided into two steps: 1) The feature extraction step, where the QRS complexes are enhanced, and 2) the detection step, where the position of the QRS complexes are found based on the feature signal and a classification procedure. Two of the commonly applied techniques for feature extraction include different variations of digital bandpass (BP) filtering [6] and wavelet decomposition [7]–[14], but several other techniques have also been proposed, e.g. morphological operators [15] or the phasor transform method [16]. Adaptive thresholding is commonly applied for the detection step [6]–[10], [13]–[15]. This method has proven robust with respect to both secure detection of abnormal beat morphologies and varying signal to noise ratios (SNRs). An extensive review of methods for software QRS detection can be found in [17]. However, many of the traditional algorithms applied in ECG analysis software today are not optimized for real-time embedded analysis. Furthermore, the location of the ePatch and the short distance between the bipolar recording sites imply that the morphology of the recorded ECGs is slightly different. The focus of this study is therefore to design, implement, and validate a novel algorithm which is optimized for automatic embedded detection of QRS complexes in patch ECGs. The requirements of the algorithm are thus high clinical performance and low computational costs.

II. METHODS AND PROCEDURES

An overview of the study is provided in Fig. 2. In the first step, we designed and optimized the algorithm using

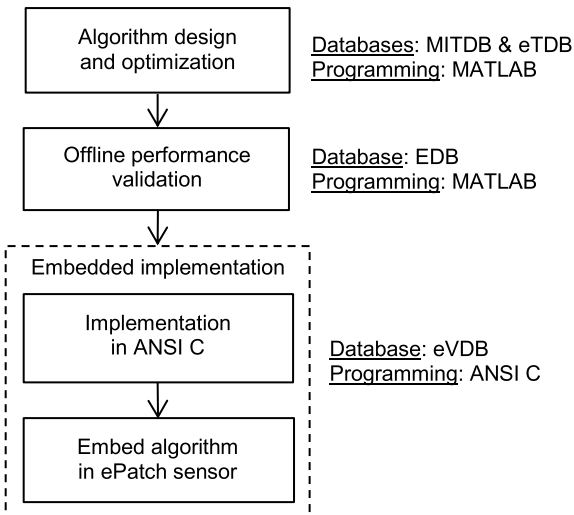


FIGURE 2. Schematic overview of the study design.

MATLAB R2013b (The MathWorks Inc., Massachusetts, USA). In the second step, we conducted an offline validation to ensure that the clinical performance on unseen data was satisfactory. The third step was to implement the algorithm in ANSI C and embed it in the ePatch sensor to allow real-time QRS detection. During the design and validation, it is important to apply ECGs with a high number of different beat morphologies from many different patients. As indicated in Fig. 2, we therefore decided to apply four different databases according to the following scheme: The design and optimization phase was based on the MIT-BIH Arrhythmia Database (MITDB) [19] and a private ePatch Training Database (eTDB). The offline validation was conducted using the European ST-T Database (EDB) [20]. Finally, the double-blinded embedded validation was conducted using the private ePatch Validation Database (eVDB). An overview of the characteristics of each database is provided in Table 1, and a detailed description is provided in the section ‘‘Data Description’’. This database selection ensures both a realistic impression of the performance on ECGs recorded with the ePatch and it allows for comparison with other published work. The algorithm is designed with special attention to overcome some of the difficulties related to the placement of the recording sites applied in the ePatch.

TABLE 1. Summary of database characteristics.

Database	Fs (Hz) ^a	Records ^b	Length (min) ^c	Beats ^d
MITDB	360	48	30	91,285
EDB	250	90	120	759,878
eTDB	512	120	10	45,248
eVDB	512	61	15	38,429

^a The original database sampling frequency (fs).

^b Total number of records in the database.

^c Entire duration of each record. Note that the first five minutes of each record is allowed as initialization time and is not included in the evaluation.

^d The total number of beats in the evaluation period of the database.

Some of the challenges include relatively large changes in signal amplitude related to changes in patient posture (including changes in QRS polarity), and cases of very pronounced P-, Q- and/or S-waves. During the design and optimization phase, priority was therefore given to improve detection performance on challenging ePatch ECGs.

A. ALGORITHM OVERVIEW

An overview of the algorithm is provided in Fig. 3. We designed the algorithm for real-time embedded functionality in a clinical setting. This was achieved by processing the ECG signal sample by sample and designing a novel cascade of simple finite impulse response (FIR) filters that allow efficient enhancement of the QRS complexes and high artefact attenuation. The input to the algorithm is one channel raw ECG. The feature extraction is indicated by the dashed green square in Fig. 3. It consists of BP filtering, removal of signs, and smoothening. The output of the feature extraction block is a feature signal (*Feature*) that is directly applied in the detection block. However, the algorithm is only allowed to continue to the detection block if the refractory period (T_{ref}) is exceeded. The refractory period serves as a simple threshold and the value is optimized in a parameter grid search described later. For the detection step, we applied two adaptive thresholds in a search back scheme. As observed from the dashed blue square in Fig. 3, the QRS detection block can therefore function in three different modes.

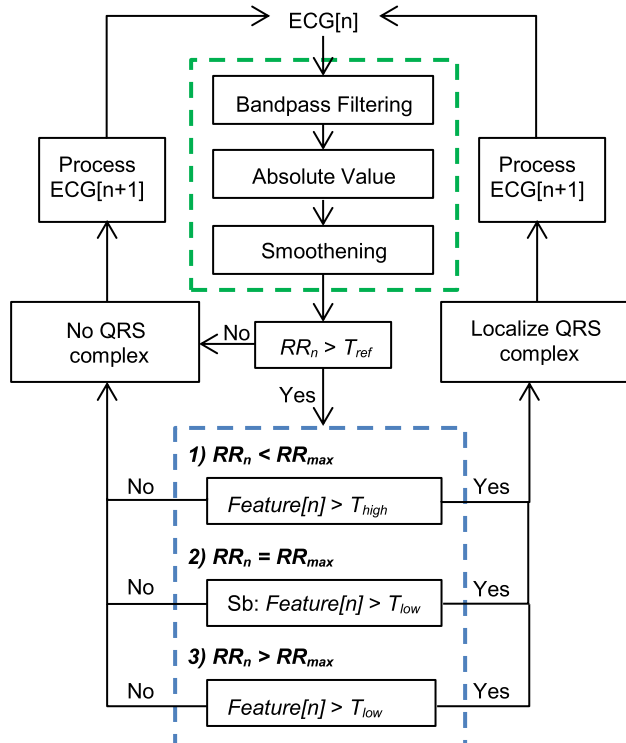


FIGURE 3. Schematic overview of the designed QRS complex detection algorithm. RR_n indicates the current RR interval, if a QRS complex is detected at the current sample, n .

The first mode applies the high threshold, T_{high} , and is active when the distance from the previous QRS detection is within the expected maximum RR interval (RR_{max}). If RR_{max} is exceeded, a search back (Sb) is performed using the low threshold value, T_{low} . This search back procedure is the second detection mode. If several samples exceed T_{low} in the search back interval, the sample with the highest *Feature* value is selected as the preliminary QRS position. If no QRS complex is detected during the search back, T_{low} is applied until a new QRS complex is detected. This is the third detection mode. The search back is a well-known procedure [6]. However, we have simplified the calculation of the adaptive thresholds to decrease the computational load, and we have refined the adaptation of the search back procedure in cases of irregular heart rhythms.

When a QRS complex is detected, a delineation procedure is applied to locate the QRS complex at the correct position, and the detection block switches back to the first mode. The following sections contain a detailed description of each part of the algorithm.

B. BANDPASS FILTERING

The purpose of the BP filtering step is two-fold: 1) Increase the influence of the QRS complexes, and 2) attenuate the influence of different types of noise, as well as pronounced P- and T-waves. However, it is also important to keep in mind that BP filtering might unintentional decrease the influence of abnormal beat morphologies, especially ventricular ectopic beats (VEBs) that are generally recognized by an increase in the width of the QRS complex. The performance of the PB filtering step is a major determinant of the necessary complexity of the remaining parts of the algorithm. It is generally accepted that the frequency components of the QRS complex primarily is between approximately 5 to 22 Hz [6], [9], [14], [15]. As mentioned, we designed a novel cascade of simple FIR filters that obtain a favorable passband in the region of the QRS complex. The cascade of filters consists of two BP filters followed by one lowpass (LP) filter. The impulse responses for the two successive BP filters are defined by (1) and (2).

$$h_{BP1}[n] = \{-\delta[n+10] - \delta[n+9] + \delta[n+2] + \delta[n+1] \\ + \delta[n] + \delta[n-1] - \delta[n-8] - \delta[n-9]\} \quad (1)$$

$$h_{BP2}[n] = \{-\delta[n+14] - \delta[n+13] + \delta[n+2] + \delta[n+1] \\ + \delta[n] + \delta[n-1] - \delta[n-12] - \delta[n-13]\} \quad (2)$$

The LP filter, with impulse response defined by h_{LP} , is an average filter with 16 points. This cascade of filters corresponds to an equivalent BP filter with impulse response h defined by (3), where $*$ is the convolution operation. The amplitude characteristics of the three individual filters, and the equivalent BP filter is provided in Fig. 4.

$$h[n] = h_{BP1}[n] * h_{BP2}[n] * h_{LP}[n] \quad (3)$$

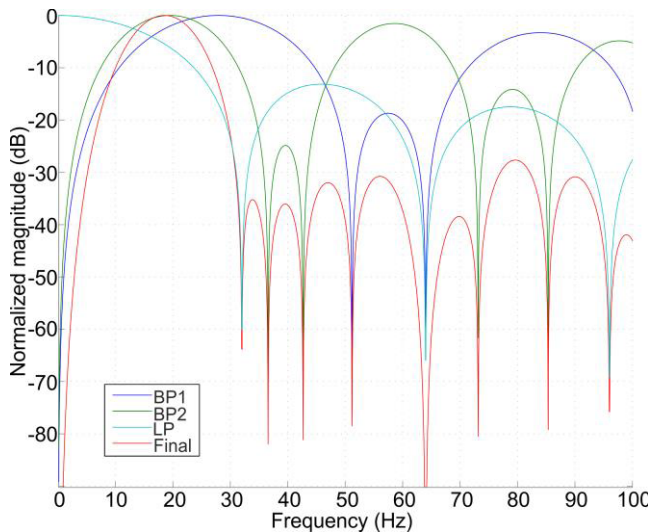


FIGURE 4. The amplitude characteristics of the three individual filters (the dark blue line represents BP1, the green line represents PB2, and the light blue line represents LP), and the resulting equivalent BP filter (red line) using a sampling frequency of 512 Hz. For frequencies above 100 Hz, the final equivalent BP filter has attenuation of at least –30 dB.

C. FINAL FEATURE EXTRACTION

The final feature signal, *Feature*, is obtained by smoothening the absolute value of the output from the BP filtered ECG signal using an 8 point FIR average filter. The absolute value is applied to ensure equal detection of QRS complexes with positive and negative polarity. As mentioned, this is especially important for ECGs recorded with the ePatch technology. An illustration of the feature extraction is provided in Fig. 5. It is observed how muscle artefacts, electrode motion artefacts, and P- and T-waves are attenuated. The total delay of all four cascaded filters is 34 samples. Using a sampling frequency of 512 Hz, this corresponds to 66.4ms,

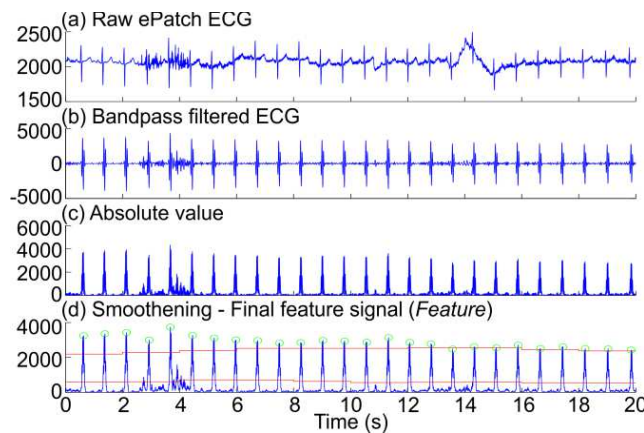


FIGURE 5. Illustration of each step in the feature extraction block:
 (a) Example of raw ECG signal recorded with the ePatch sensor. The amplitude is illustrated in analog-to-digital count (ADC) values for all plots. Note the presence of both muscle artefacts and electrode motion artefacts. (b) The ECG signal after BP filtering using the novel cascade of simple filters. (c) Absolute value of the BP filtered ECG signal. (d) Smoothing of the feature signal. The red lines indicate T_{high} and T_{low} . The green circles indicate the detected positions of the QRS complexes.

which we considered to be within the acceptable limit for clinical applications.

D. THE QRS DETECTION BLOCK

As mentioned, the QRS detection block consists of two adaptive thresholds that are applied in a search back manner. One of the important components in such an algorithm is timely initiation of the search back procedure. This initiation is decided by the maximum expected RR interval between two subsequent QRS complexes, RR_{max} . The assumption in this study was that RR_{max} should vary with the general variation of the RR intervals. The timely initiation of the search back procedure is especially important in the presence of abnormal beats that might not be detected using T_{high} . In many cases, it is therefore advantageous to initiate the search back procedure earlier in a recording with high variability in the RR intervals. The algorithm was therefore designed to function in two different variability modes (low variability and high variability) described below.

1) ESTIMATION OF THE OPTIMAL VARIABILITY MODE

To estimate the optimal variability mode, the 34 most recently detected RR intervals are saved in a vector termed RR_{long} . The current variability parameter, θ , is then estimated as:

- 1) Calculate the median of RR_{long} .
- 2) Calculate the absolute deviation between each RR interval in RR_{long} and the median. The deviation vector is termed ε .
- 3) Remove the two largest values from ε .
- 4) θ is then defined as the mean value of the remaining 32 entries in ε .

The third step is included to prevent a single ectopic beat detection, a single missed detection, or a single false positive from pushing the algorithm in the high variability mode. This mode is only intended to be activated for records with many ectopic beats or generally high variation in the RR intervals, e.g. cases of AF. In these records, it is expected that the risk of missing a beat is increased, and to prevent this, the “sensitivity” of the search back is increased. It is important that RR_{long} contains enough RR intervals to provide a reliable estimate of the current RR variability. At the same time, it is important that RR_{long} is adaptive and hereby able to change relatively fast when the heart rhythm changes. This requires a shorter history of the RR intervals. We therefore found that 34 RR intervals was a good compromise. The high and low variability modes are defined based on θ being above or below a threshold, T_θ . The threshold was set to $T_\theta = 35$ samples. This was obtained by visual inspection of the time course of θ calculated from the reference annotations from the MITDB relative to the heart rhythms that are intended to initiate the high variability mode.

2) ESTIMATION OF THE EXPECTED MAXIMUM RR INTERVAL (RR_{max})

RR_{max} is calculated according to (4) and (5), where \tilde{x} is the median value of the elements in x , $Min(x)$ is the

minimum value of the elements in x , RR_{scale} is a scaling parameter, RR_{short} contains the 8 previously detected RR intervals (RR_{short} can be derived directly from RR_{long} , but it contains a shorter history and is thus faster adapted to changes in the heart rhythm), and $RR_{searchback}$ contains the 8 previously detected RR intervals that were detected during search back (this ensures that information about the general RR intervals during previous episodes of search back is saved). In the low variability mode, RR_{long} provides a good estimate of the expected RR interval. In the high variability mode, the minimum of the two more sensitive RR variables is used to increase the search back sensitivity. The median value is applied to avoid high influence of a single false high or low RR interval. RR_{max} and θ are updated every two seconds together with the adaptive thresholds.

$$RR_{temp} = \begin{cases} \widetilde{RR_{long}} & \text{if } \theta \leq T_\theta \\ \text{Min}(\widetilde{RR_{short}}, \widetilde{RR_{searchback}}) & \text{if } \theta > T_\theta \end{cases} \quad (4)$$

$$RR_{max} = RR_{temp} \cdot RR_{scale}. \quad (5)$$

3) ADAPTIVE THRESHOLDING

The purpose of adaptive thresholding is to obtain thresholds that follow the changes in the signal. This is especially important for analysis of ePatch ECG signals. The goal is to obtain smooth adaptation to changes in both ECG signal amplitude and changes in the amount and types of artefacts. We decided to update the threshold parameters in non-overlapping windows of two seconds. This ensures the presence of at least one QRS complex in each window within the normal heart rate range. The high threshold, T_{high} , is based on the median of the maximum feature value in the eight previous windows:

$$T_{high}[m] = (\max_{F[m-8]} \dots \max_{F[m-1]}) \cdot \widetilde{\alpha}. \quad (6)$$

In (6), m indicates the window number, $F[m]$ represents the final feature signal in window m , \max_x is the maximum value of the elements in x , and α is a scaling factor slightly lower than 1. In most cases, the maximum value of a two second ECG segment is expected to represent the amplitude of a QRS complex. T_{high} is thus designed to float right below the expected amplitude of the QRS complexes.

The low threshold, T_{low} , is intended to adjust faster to rapid changes in the amount of artefacts. This threshold is therefore based on information about the mean value of the final feature signal in the two previous windows. It is known that an increase in heart rate induces an increase in the mean value of the feature signal. T_{low} is not intended to increase as a consequence of increased heart rate. Therefore, T_{low} is scaled according to the number of QRS detections obtained in the two successive windows applied for the threshold calculation. This modification is termed s_1 . The s_1 parameter is furthermore bounded as follows:

- 1) If no QRS complexes were detected, set $s_1 = 1$.
- 2) If > 8 QRS complexes were detected, set $s_1 = 8$.

It is furthermore important to note that episodes of very noisy segments might disturb the QRS detection and produce

a number of false positive detections that might induce RR variability similar to e.g. episodes of AF. To prevent the increased sensitivity of the search back procedure from exacerbating the number of false positive detections in noisy data, a modification of T_{low} is also needed in the high variability mode. Therefore the s_2 parameter is defined as:

$$s_2 = \begin{cases} 10 & \text{if } \theta \leq T_\theta \\ 12 & \text{if } \theta > T_\theta \end{cases}. \quad (7)$$

These values were obtained by visual inspection of different challenging ECG snippets from the training data (MITDB and eTDB). The temporary low threshold, $T_{low,temp}$, is thus calculated by (8), where μ_x is the mean value of the elements in x .

$$T_{low,temp}[m] = (\mu_{F[m-2]}, \mu_{F[m-1]}) \cdot \frac{\widetilde{s_2}}{s_1}. \quad (8)$$

Finally, T_{low} is furthermore bounded by a percentage, β , of T_{high} . This is defined in (9). This ensures a proper functionality of T_{low} to detect beats missed by T_{high} :

$$T_{low} = \begin{cases} T_{low,temp} & \text{if } T_{low,temp} \leq T_{high} \cdot \beta \\ T_{high} \cdot \beta & \text{if } T_{low,temp} > T_{high} \cdot \beta \end{cases} \quad (9)$$

4) QRS LOCALIZATION AND REFRACTORY BLANKING

The preliminary QRS location is the first sample where the feature signal exceeds the relevant threshold. However, this point is probably not the location of the R peak. To allow better delineation, a search is performed for the absolute maximum point in the final feature signal for a period of time after the exceedance of the threshold. The sample point that obtains the maximum absolute feature value during this time interval was selected as the QRS position. The search period is chosen to be equal to the refractory period (T_{ref}), in which detection of a new QRS complex is not allowed.

E. DATA DESCRIPTION

As mentioned, we applied four different databases to ensure thorough evaluation of the algorithm performance. An overview of the different databases is provided in Table 1, whereas this section contains a detailed description. For all four databases, only the first ECG channel was applied.

The eTDB was generated by extracting 10 minute ECG segments from two large existing ePatch databases. The first original database contains recordings from patients admitted to the stroke unit at Glostrup Hospital. The second original database contains ECG recordings from patients undergoing ambulatory diagnosis for obstructive sleep apnea at Glostrup Hospital. Each ECG recording in the two databases was associated with an ECG analysis report (similar to a traditional Holter analysis report). The databases were anonymous and included no personally identifiable data that could allow an individual patient to be identified. It was important to include ECG recordings from many different patients. We therefore selected 30 patients from the stroke unit database and 30 patients from the ambulatory database. It was furthermore important to ensure

representation of many different abnormal beat morphologies as well as normal sinus rhythm with different ventricular frequencies. To ensure this, we selected the 60 patients based on the summaries in the associated ECG analysis reports. From the selected patients, we extracted a total of 120 ECG segments of which 40% were selected randomly and the remaining 60% were selected based on markings of interesting data segments in the analysis reports. This segment extraction ensures a database with realistic amounts of artefacts as well as representation of many different types of abnormal beat morphologies. Some examples of included arrhythmia events are: Atrial fibrillation (AF), episodes of supraventricular tachycardia with different frequencies, supraventricular ectopic beats (SVEBs), runs of SVEBs, VEBs, ventricular bigeminy, ventricular trigeminy, bradycardia, and AV blocks.

The eVDB was generated from three ECG recordings obtained from three different healthy volunteers. The three volunteers provided informed consent before they participated in the study. They continued normal daily life activities throughout the recordings. The embedded algorithm output was calculated in real-time during the recordings, and saved in a special channel in the data file. The algorithm output was not investigated before the manual annotation of the eVDB. For each subject, a 15 minute segment was automatically extracted from minute 30 to 45 in each hour of the recording. The mean recording time was 21.0 hours, yielding a total of 20-21 segments for each subject. This ensures representation of realistic amounts of normal daily life activities and provides an overview of a potential change in performance during the recording period.

The ePatch reference annotations were created based on manual corrections of the output from the “sqrs” function from the WFDB Toolbox [21]. The manual corrections were conducted by a biomedical engineer with experience in ECG interpretation. All beats were labelled as normal. To validate the annotation performance of the biomedical engineer, 12 randomly selected records from the eTDB (10%) were also annotated by a medical doctor. The medical doctor did not find any errors in the manual annotations conducted by the biomedical engineer. The manual corrections were conducted using the WAVE program from the WFDB Toolbox [21].

The MITDB and EDB were downloaded from Physionet [21]. To obtain similar sampling frequencies for all databases, the recordings from the MITDB and EDB were resampled to 512 Hz using the “xform” function from the WFDB Toolbox [21], and they were converted to mat-files using the WFDB Toolbox for MATLAB [21]. All beats in both databases are manually labelled according to the beat type. This allows evaluation of the detection performance with respect to different abnormal beat types.

F. EVALUATION OF QRS DETECTION PERFORMANCE

The QRS detection performance was evaluated as the QRS sensitivity ($Se = TP/(TP + FN)$) and positive predictivity

($P^+ = TP/(TP + FP)$), where TP is the number of true positive detections, FP is the number of false positive detections, and FN is the number of false negative detections (missed QRS complexes). In compliance with [22], TP, FP, and FN for each record, were calculated using the default settings of the “xbx” function from the WFDB toolbox. This implies that the first five minutes of each record is allowed as a training period and episodes of ventricular flutter or fibrillation (VF) were excluded [21]. The performance for each database is stated as gross statistics [22]. No records were excluded in the performance evaluation.

G. EVALUATION OF EMBEDDED ALGORITHM PROCESSING TIME

After the offline validation, the algorithm was implemented in ANSI C, compiled and embedded in the ePatch sensor. The sensor has a 32 bit micro controller based on the ARM Cortex-M3 processor from Energy Micro (now acquired by Silicon Labs). A low processing time for each sample allows the processor to enter “sleep” mode and hereby save energy. Furthermore, it is important that the processing time of each sample will never exceed the time between two samples. The processing time for each sample will among other things depend on the algorithm mode applied for that specific sample and whether a QRS complex is detected or not. Furthermore, every two seconds the thresholds and other adaptive parameters are updated. This will clearly require more processor time than processing a non-boundary ECG sample between two QRS complexes. We therefore decided to investigate the processing time using a histogram. The histogram was created with a clock cycle counter that counted how many clock cycles the algorithm spends on processing each sample in a real-life recording. The duration of the recording was approximately 2.3 hours, yielding a total of 4,271,185 samples.

III. RESULTS

A. ALGORITHM PARAMETER OPTIMIZATION

Four of the algorithm parameters were chosen based on a parameter grid search on the training databases (MITDB and eTDB). The four parameters were the refractory blanking period ($T_{ref} = 0.2s, 0.25s, \text{ or } 0.3s$), the scaling of the expected RR interval ($RR_{scale} = 1, 1.2, \text{ or } 1.3$), the boundary for T_{low} ($\beta = 0.4, 0.5, \text{ or } 0.6$), and the scaling parameter for T_{high} ($\alpha = 0.8, 0.9, \text{ or } 0.99$). The investigated values were selected based on clinical relevance, theoretical sense, and experience from the literature. The parameters are mutually dependent on each other. Therefore, the performances of all 81 different combinations of parameter values were investigated. The relationship between Se and P^+ for all 81 combinations is provided in Fig. 6. The selected parameter combination was $T_{ref} = 0.25s$, $RR_{scale} = 1.2$, $\alpha = 0.8$, and $\beta = 0.4$.

B. QRS DETECTION PERFORMANCE

With the selected parameter combination, the obtained Se and P^+ on the eTDB was 99.88% and 99.37%, respectively. The performance obtained on the MITDB and the

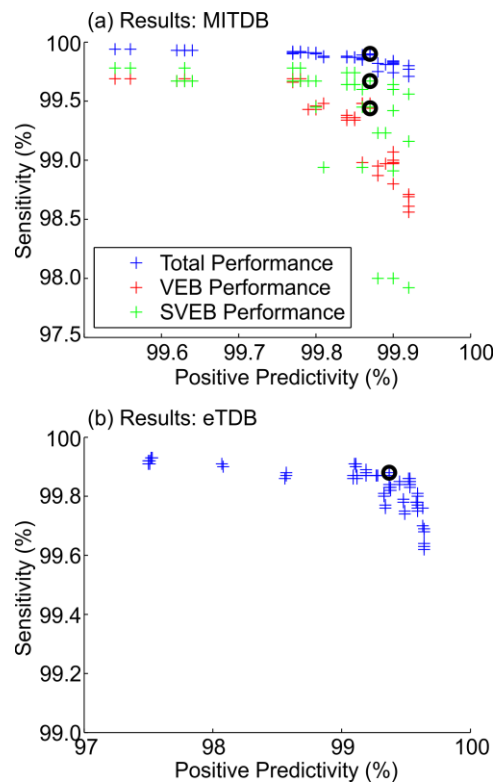


FIGURE 6. Relation between P^+ and Se for (a) the MITDB and (b) the eTDB. Each mark indicates the performance for one of the 81 investigated parameter combinations. In (a), the blue marks indicate performance on the entire database, the green marks indicate Se on SVEB beats only, and the red marks indicate Se on VEB beats only. In compliance with [22], the SVEB beat category includes atrial and nodal premature and escape beats and aberrated premature atrial beats. Likewise, the VEB beat category includes ventricular premature beats, R-on-T ventricular premature beats, and ventricular escape beats [22]. The black circles indicate the parameter combination that was selected for further embedded implementation. Note, that the axes are zoomed to allow a better view of each point.

TABLE 2. QRS detection performance on the MITDB and the EDB.

Method	MITDB		EDB	
	P^+ (%)	Se (%)	P^+ (%)	Se (%)
This work [#]	99.87	99.90	99.71	99.84
Di Marco and Chiari [7]	99.86	99.77	99.56	99.81
Ghaffari et al. [13]	99.88	99.91	99.55	99.63
Ghaffari et al. [14]	99.91	99.94	-	-
Liu et al. [10] ^{\$}	99.86	99.80	-	-
Li et al. [11] ⁺	99.94	99.89	-	-
Martinez et al. [16]	99.97	99.71	99.73	99.67
Martinez et al. [12]	99.86	99.80	99.48	99.61
Zhang and Bae [15] *	99.82	99.76	-	-
Pan and Tompkins[6] ^{++#}	99.54	99.75	-	-
Zidelman et al. [9]	99.82	99.64	-	-

⁻ Not stated in paper.

[#] Algorithm is implemented and tested in a microprocessor.

^{\$} Algorithm is implemented and tested on an ASIC.

^{*}Algorithm is implemented and tested on a FPGA.

⁺A discrepancy was found between the stated total number of beats and the record-by-record total number of beats. In this table, the record-by-record numbers are applied.

EDB using this parameter combination is provided in Table 2. Table 2 furthermore contains examples of the performance on these databases reported in the literature. To further compare

the performance of the proposed algorithm with other published work, we conducted Mann-Whitney U tests (the data is not normally distributed). However, this statistical significance test is only possible when the performances on each record are stated individually in the published papers. This was the case for [6], [9], [11], and [15] on the MITDB, and unfortunately no papers on the EDB. We applied the *ranksum* function in MATLAB R2013b and a significance level of 0.05. We found that the median of both Se and P^+ of the proposed algorithm are significantly higher than the median Se and P^+ obtained by [6], [9] and [15]. On the other hand, the test showed no statistical significant difference between the median performances obtained by the proposed algorithm and [11]. It should be noted that the individual performances obtained on record 214 and 215 were not stated by [11]. These records were therefore excluded when comparing with [11].

For the EDB, Se with respect to detection of QRS complexes from the overall beat categories VEB and SVEB (see Fig. 6 for definitions [22]) was 97.60% and 99.53%, respectively. The reference annotations from the MITDB have a quite detailed separation between different clinically relevant beat types (of which some are subtypes of the overall categories VEB and SVEB). For the MITDB, we therefore state the detection performance for the overall beat categories VEB and SVEB as well as the performance on a few selected clinically relevant individual beat types. These sensitivities are provided in Table 3.

TABLE 3. Sensitivity of QRS detection on the MITDB with respect to different types of abnormal beat morphologies.

Beat type	VEB ^a	PVC ^b	SVEB ^c	PAC ^d	LBBB ^e
Se (%)	99.44	99.43	99.67	99.91	99.96

^a See Fig. 6 for a definition of all included beat types in this category.

^b Premature Ventricular Contractions (indicated by “V” in the MITDB reference annotations). This is a subtype of the VEB category.

^c See Fig. 6 for a definition of all included beat types in this category.

^d Premature Atrial Contractions (indicated by “A” in the MITDB reference annotations). This is a subtype of the SVEB category.

^e Left Bundle Branch Block (indicated by “L” in the MITDB reference annotations). These beats are not included in the SVEB or VEB categories.

The results from the double-blinded performance evaluation on the eTDB are provided in Table 4. The performance is stated for both the MATLAB code, the offline C code, and the embedded code. This allows comparison between the three implementations.

C. QRS DETECTION EXAMPLES

Fig. 7 illustrates the algorithm performance in different challenging clinically relevant cases from the eTDB.

Fig. 7 (a) illustrates two interesting issues: 1) Very pronounced P-waves with high slopes, and 2) a run of SVEBs/sudden tachycardia onset. It is observed that all QRS complexes are correctly detected by the algorithm. This is obtained through a timely initiation of the search back procedure for all QRS complexes in the SVEB run with amplitude

TABLE 4. Performance of the double-blinded validation of the QRS detection algorithm on the eVDB.

Subject	Records ^a	Beats ^b	MATLAB		Offline C code		Embedded	
			Se (%)	P ⁺ (%)	Se (%)	P ⁺ (%)	Se (%)	P ⁺ (%)
Subject1	20	11,510	99.83	99.72	99.83	99.72	99.83	99.72
Subject2	20	12,396	99.99	99.85	100	99.86	100	99.86
Subject3	21	14,523	99.92	99.80	99.91	99.79	99.89	99.80
Total	61	38,429	99.92	99.79	99.92	99.79	99.91	99.79

^aThe number of records extracted from each healthy test subject.

^bThe total number of beats in the evaluation period for each test subject.

lower than T_{high} (indicated by black circles). This illustrates the high adaptability of the search back initiation in this algorithm. It is furthermore observed that the QRS complexes after the SVEB run are detected using T_{low} in the third algorithm mode (magenta circles). This occurs because it requires some time to adapt to the slower heart rate by decreasing the sensitivity of the search back procedure again. The pronounced P-waves are also observed in the final feature signal. In cases using T_{high} , this is not problematic. In cases using the search back procedure or T_{low} , this could induce false detections of the P-wave when they exceed T_{low} . However, the localization block is observed to correctly prevent false detections of the P-wave for all QRS complexes.

Fig. 7 (b) illustrates a case of AF with VEBs. The VEBs are wider, and therefore less pronounced in the final feature signal. This is, again, not problematic due to timely initiation of the search back procedure in the VEB positions (black circles). It is furthermore observed that the normal beats after two of the VEBs are detected in the third algorithm mode (magenta circles). In these two cases, the algorithm thus proves to function exactly as intended. At fourteen seconds, one QRS complex is detected using the search back mode even though the amplitude exceeds T_{high} . This is due to a very sensitive search back that is initiated on the rising slope of the QRS complex. The localization block is then initiated from the search back procedure and ensures correct localization of the QRS complex. The high search back sensitivity for this recording is caused by the characteristic irregularity of the RR intervals that is observed during episodes of AF.

Fig. 7 (c) illustrates the performance during a sudden change in amplitude. It is observed how T_{high} is quickly adapted to the new level of the QRS complexes. Even in the meantime, no QRS complexes are missed due to the correct functionality of the search back procedure. This feature of the algorithm is very important in real-life clinical applications where patients would wear the ePatch during normal daily life activities for extended periods of time. Furthermore, it is observed that the minor muscle and motion artefacts present in Fig. 7 (c) does not disturb the automatic QRS detection.

D. EMBEDDED PROCESSING TIME

The histogram of the processing times for a real-life recording is provided in Fig. 8. Two distinct peaks are observed from the histogram. The first peak represents samples with

a processing time between $30\mu s$ and $90\mu s$. This peak corresponds to processing of a non-boundary sample. The smaller peak represents samples with processing times between $120\mu s$ and $240\mu s$. This corresponds to samples lying on a two second boundary where all the adaptive parameters are updated. It is furthermore observed that no sample has a processing time of more than $240\mu s$. Furthermore, 99.82% of the recorded samples belong to the second histogram bin. To provide a theoretical estimate of the worst case energy consumption, we therefore apply the upper limit of this bin corresponding to a processing time of $60\mu s$. This implies that we expect the algorithm to be active in less than 3.07% of the time with a sampling frequency of 512Hz. This allows the processor to enter sleep mode or perform other activities for almost 97% of the time. The typical energy consumption of the processor is 5.62mA. Theoretically, the algorithm thus uses up to 0.1726mA. During normal operation (recording, sampling, storage etc.) the ePatch sensor uses 3.125mA. This implies that the algorithm causes a theoretical worst case increase in the energy consumption compared to the normal ePatch sensor activity of 5.5%. This corresponds to a decrease from a maximum recording time of 80 hours to a maximum recording time of 75.8 hours using a 250mAh battery.

IV. DISCUSSION

On the MITDB, we obtained a sensitivity and positive predictivity of 99.90% and 99.87%, respectively. This performance is comparable to the best results obtained in the literature (see Table 2). These results [13], [14] are, however, not obtained by an embedded algorithm that have been tested in real-life situations. When compared to [6] and [15] that are examples of other embedded algorithms, the performance obtained by our novel algorithm is significantly higher. The sensitivity with respect to detection of abnormal beat morphologies was unfortunately not stated by the other authors, which makes comparison impossible. However, we consider our detection sensitivity with respect to different abnormal beat morphologies to be high. This is especially relevant if the algorithm is intended to be applied in a clinical setting. In a clinical setting, it can be imagined that the automatic QRS complex detection algorithm works as a pre-processor or initiator of a beat or event classification procedure. This could be highly relevant in applications like tele-monitoring, “admission” of patients in their own home, or rehabilitation programs. Reliable products that can manage tasks

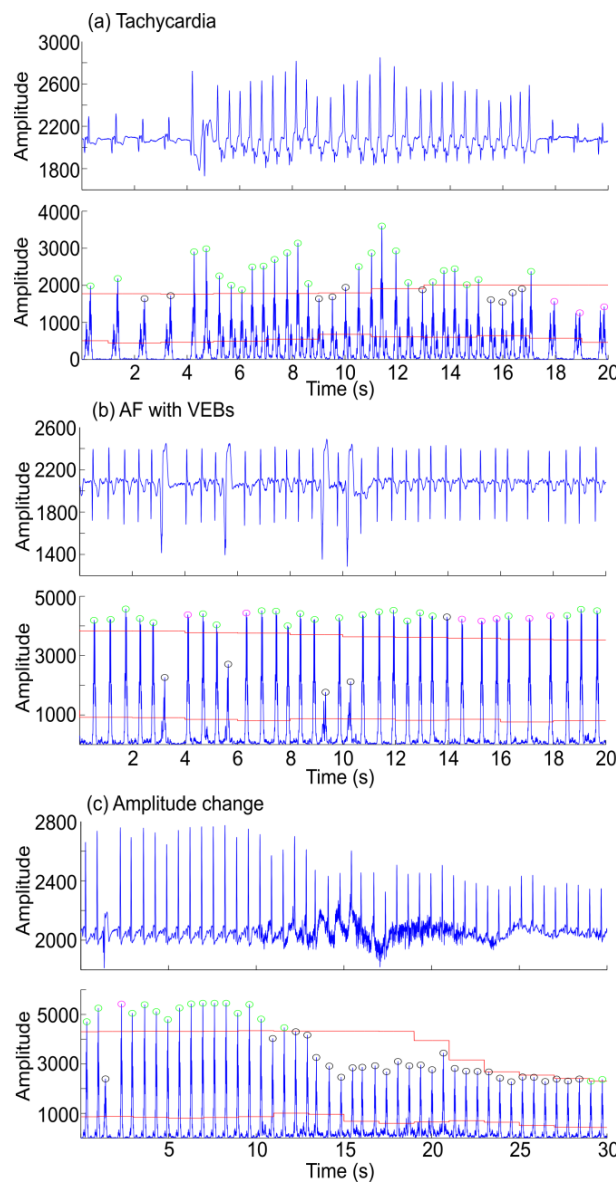


FIGURE 7. Illustration of performance on three challenging cases from the eTDB: (a) Sudden onset of tachycardia, (b) AF with VEBs, and (c) sudden change in amplitude. The top plot in each subfigure is one channel of raw ECG. The amplitude is illustrated in analog-to-digital counts (ADC). The bottom plot in each subfigure is the final feature signal (blue line) together with T_{high} and T_{low} (red lines). The green circles indicate QRS positions detected using T_{high} (mode 1), the black circles indicate QRS positions detected during search back (mode 2), and the magenta circles indicate QRS complexes detected using T_{low} (mode 3).

like these could highly increase the diagnosis and treatment of many different groups of patients. It should, of course, be mentioned that many different clinically relevant abnormal beat types and arrhythmias exists and the evaluation of our algorithm on abnormal beat morphologies is therefore not exhaustive.

On the EDB, we obtained a sensitivity and positive predictivity of 99.84% and 99.71%, respectively. This performance is among the highest performances stated in the literature

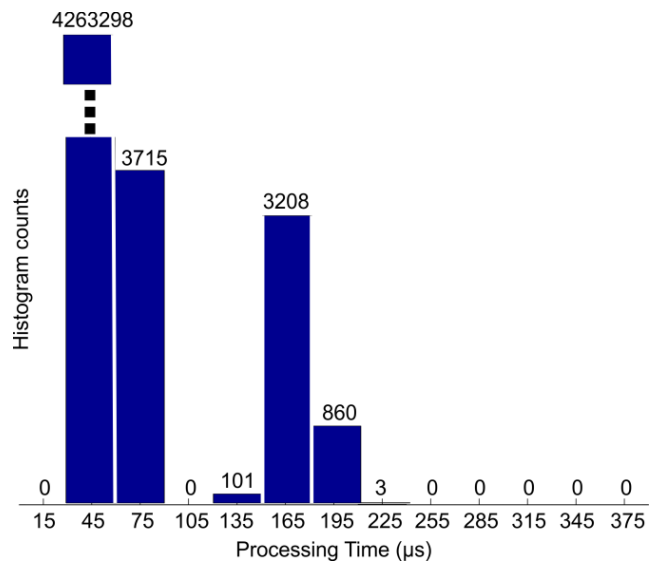


FIGURE 8. Histogram of the embedded algorithm processing time for each sample in a real-life recording of 2.3 hours. The x-axis indicates the center value of each histogram bin. This implies that the first bin contains samples with a processing time of 0-30 μ s, the second bin contains samples with a processing time of 30-60 μ s etc.

for this database. It should furthermore be noted that this database was used only as a validation database. This implies that the algorithm design and parameter selection was not changed prior to the processing of this database. This result can thus provide a relatively realistic impression of the performance on unseen ECG signals with different types of abnormal beat morphologies from a large number of different patients.

The sensitivity ($Se = 99.88\%$) on the eTDB is also considered to be very high. The positive predictivity ($P^+ = 99.37\%$) is, however, slightly lower than for the other databases. This is primarily caused by low P^+ in two records from the same patient. These records contain ECG data of relatively poor quality. The rhythm is AF, and the fibrillating “P-waves” are very pronounced compared to the QRS complexes. These records were, however, included in the study to ensure that the parameter optimization would be more realistic.

Furthermore, the performance in the double-blinded validation of the embedded algorithm is also considered superior ($Se = 99.91\%$ and $P^+ = 99.79\%$). This demonstrates how the algorithm can obtain a high performance throughout a long-term recording with artefacts from normal daily life activities. Furthermore, there is no significant difference between the performances obtained by the three implementations of the algorithm.

From the literature it is observed that especially the wavelet decomposition method has been investigated with good performance in a high number of studies. The difference equations for implementation of the commonly applied *a trous* wavelet scheme can be found in [10]. The computational complexity of the proposed novel cascade of filters is similar

to the traditional *a trous* wavelet decomposition. However, using the wavelet decomposition, the relevant frequencies of the QRS complex is often divided across several wavelet detail sub-bands. Therefore, a combination of the information in several different sub-bands is usually required when applying the wavelet technique [7]–[14]. This combination of information requires additional computations. Furthermore, the application of the wavelet transform often requires additional blocks after the wavelet decomposition to obtain satisfactory enhancement of the QRS complexes or to confirm a QRS candidate. This includes for instance calculation of maximum-minimum-difference [7], confirmation of zero-crossings [8], multiplication of detail coefficients from selected scales [9], [10], denoising of wavelet output [10], detection of modulus-maxima exceeding thresholds in several detail bands [11], [12], calculation of area-curve length [13], [14], normalization using standard deviation [14], and non-linear exponential amplification of the feature signal [14]. These additional algorithm steps decrease the computational efficiency of the algorithms. The desired low computational burden associated with our algorithm is obtained partly by the novel cascade of simple FIR filters. The output from these filters is a feature signal that is smooth enough to allow direct detection of QRS complexes using only two adaptive thresholds. However, it should be noted that many studies have also obtained high performance in P- and T-wave delineation using the wavelet transform. If the intended application requires this delineation, it should therefore be investigated whether the decreased computational load in our QRS complex detection algorithm might be outweighed when P- and T-wave delineation is included. However, the influence of this depends highly on the intended application of the QRS complex detection algorithm and the features selected for subsequent potential arrhythmia and event classification.

The application of two adaptive thresholds and timely initiation of the search back procedure is another advantage of our algorithm. This design decreases the algorithm sensitivity with respect to detection of noise events without decreasing the sensitivity with respect to detection of abnormal beats. The idea of increasing algorithm sensitivity when irregular RR intervals is observed was already suggested by [6]. However, we propose a different solution where the algorithm sensitivity is increased directly by fast adjustments of RR_{max} instead of decreasing the detection thresholds. This method increases the likelihood of detecting premature beats. Using this method, it is possible to obtain high clinical detection performance without application of computationally costly thresholds.

The superior performance of the algorithm observed from the challenging, but clinically very relevant cases in Fig. 7 is promising. Furthermore, the performance in the double-blinded validation and on the standard databases is considered very high. This high clinical performance is obtained using an algorithm that is simple enough for embedded real-time implementation in the ePatch sensor. This is also illustrated

in Fig. 8: 99.82% of the samples are processed in less than $60\mu s$. Even every two seconds when a boundary is reached and the adaptive algorithm parameters are updated, the maximum processing time is $240\mu s$. This feature is very attractive since it allows the processor to enter “sleep” mode and hereby save energy. Furthermore, it leaves valuable overhead for the recording functionality and processing of other potential embedded algorithms in future applications.

It should be noted that future work could include specific noise stress tests of the algorithm. In our study, we include artefacts from normal daily life activities (especially in the eVDB), but the performance of the algorithm during specific types and amounts of artefacts could be further investigated. In extremely noisy data segments there is always a risk of obtaining a high number of FP or FN detections. This might disturb the adaptive parts of the algorithm and exacerbate a poor performance. This could be accounted for in future versions of the algorithm. This improvement could for instance include a pre-qualification of the signal quality that could decide whether the adaptive parameters should be updated, or it could include hard boundaries on the adaptive parameters. A compensation for this could furthermore include a possibility of resetting the adaptive parameters when it is detected that the previous data segment was very noisy. However, the amount of noise needs to be very pronounced for a longer period of time before this becomes problematic.

It should also be noted that the algorithm can produce some FP detections during episodes of AF if the baseline is very influenced by the unorganized electrical activity of the atria. Due to the placement of the ePatch, this atrial activity during episodes of AF is sometimes very pronounced on ECG recorded with the ePatch. This is actually expected to be an advantage for heart rhythm analysis, but it might increase the difficulty of automatic QRS complex detection. However, a few false detections during episodes of AF are not expected to disturb subsequent automatic rhythm analysis and automatic classification of AF versus other heart rhythms. The characteristic irregularity of the RR intervals during AF is still expected to be clearly observed in case of a few FP detections.

Our overall impression is that this novel algorithm is very relevant in clinical applications. The high performance on both normal and abnormal beat morphologies and the possibility of embedded implementation opens possibilities of real-time monitoring of clinically relevant parameters like heart rate, rhythm analysis, and detection of cardiac events on patients outside the hospital.

V. CONCLUSION

We have designed a computationally efficient algorithm for real-time automatic QRS complex detection. The performance of the algorithm has been validated on ECG signals from two large standard databases and two private ePatch databases (MITDB: $Se = 99.90\%$, $P^+ = 99.87$, EDB: $Se = 99.84\%$, $P^+ = 99.71\%$, eTDB: $Se = 99.88\%$,

$P^+ = 99.37\%$, and eVDB: $Se = 99.91\%$, $P^+ = 99.79\%$). Together, these four databases contain a high number of abnormal beat morphologies, normal sinus rhythm with different ventricular frequencies, and different amount of artefacts originating from daily life activities. The performance of the algorithm is thus considered high enough for clinical application of the embedded algorithm in the ePatch ECG recorder. The implementation of automatic ECG analysis functionality in small wearable patch type ECG recorders is expected to highly increase the possibilities of early diagnosis, timely treatment, and regular follow-up on patients with life threatening heart diseases like AF.

ACKNOWLEDGMENT

The authors wish to thank the clinical staff at Glostrup Hospital for conducting the clinical ePatch recordings and creating the Holter analysis reports that were applied for the selection of the database.

REFERENCES

- [1] World Health Organization. (2013). *Cardiovascular Diseases (CVDs)*. [Online]. Available: <http://www.who.int/mediacentre/factsheets/fs317/en/>, accessed Jan. 24, 2014.
- [2] M. P. Turakhia *et al.*, "Diagnostic utility of a novel leadless arrhythmia monitoring device," *Amer. J. Cardiol.*, vol. 112, no. 4, pp. 520–524, Aug. 2013.
- [3] D. B. Saadi *et al.*, "Heart rhythm analysis using ECG recorded with a novel sternum based patch technology—A pilot study," in *Proc. Int. Congr. Cardiovascular Technol. (CARDIOTECHNIX)*, 2013, pp. 15–21.
- [4] M. A. Rosenberg, M. Samuel, A. Thosani, and P. J. Zimetbaum, "Use of a noninvasive continuous monitoring device in the management of atrial fibrillation: A pilot study," *Pacing Clin. Electrophysiol.*, vol. 36, no. 3, pp. 328–333, Mar. 2013.
- [5] P. M. Barrett *et al.*, "Comparison of 24-hour Holter monitoring with 14-day novel adhesive patch electrocardiographic monitoring," *Amer. J. Med.*, vol. 127, no. 1, pp. 95.e11–95.e17, Jan. 2014.
- [6] J. Pan and W. J. Tompkins, "A real-time QRS detection algorithm," *IEEE Trans. Biomed. Eng.*, vol. BME-32, no. 3, pp. 230–236, Mar. 1985.
- [7] L. Y. Di Marco and L. Chiari, "A wavelet-based ECG delineation algorithm for 32-bit integer online processing," *Biomed. Eng. Online*, vol. 10, p. 23, Apr. 2011.
- [8] D. B. Nielsen, K. Egstrup, J. Brænbjerg, G. B. Andersen, and H. B. D. Sorensen, "Automatic QRS complex detection algorithm designed for a novel wearable, wireless electrocardiogram recording device," in *Proc. Annu. Int. Conf. IEEE Eng. Med. Biol. Soc.*, Aug./Sep. 2012, pp. 2913–2916.
- [9] Z. Zidelmal, A. Amirou, M. Adnane, and A. Belouchrani, "QRS detection based on wavelet coefficients," *Comput. Methods Programs Biomed.*, vol. 107, no. 3, pp. 490–496, Sep. 2012.
- [10] X. Liu, Y. Zheng, M. W. Phyu, B. Zhao, M. Je, and X. Yuan, "Multiple functional ECG signal processing for wearable applications of long-term cardiac monitoring," *IEEE Trans. Biomed. Eng.*, vol. 58, no. 2, pp. 380–389, Feb. 2011.
- [11] C. Li, C. Zheng, and C. Tai, "Detection of ECG characteristic points using wavelet transforms," *IEEE Trans. Biomed. Eng.*, vol. 42, no. 1, pp. 21–28, Jan. 1995.
- [12] J. P. Martínez, R. Almeida, S. Olmos, A. P. Rocha, and P. Laguna, "A wavelet-based ECG delineator: Evaluation on standard databases," *IEEE Trans. Biomed. Eng.*, vol. 51, no. 4, pp. 570–581, Apr. 2004.
- [13] A. Ghaffari, M. R. Homaeinezhad, M. Akraminia, M. Atarov, and M. Daevaeiha, "A robust wavelet-based multi-lead electrocardiogram delineation algorithm," *Med. Eng. Phys.*, vol. 31, no. 10, pp. 1219–1227, Dec. 2009.
- [14] A. Ghaffari, M. R. Homaeinezhad, and M. M. Daevaeiha, "High resolution ambulatory Holter ECG events detection-delineation via modified multi-lead wavelet-based features analysis: Detection and quantification of heart rate turbulence," *Expert Syst. Appl.*, vol. 38, no. 5, pp. 5299–5310, May 2011.
- [15] C. F. Zhang and T.-W. Bae, "VLSI friendly ECG QRS complex detector for body sensor networks," *IEEE J. Emerg. Sel. Topics Circuits Syst.*, vol. 2, no. 1, pp. 52–59, Mar. 2012.
- [16] A. Martínez, R. Alcaraz, and J. J. Rieta, "Application of the phasor transform for automatic delineation of single-lead ECG fiducial points," *Physiol. Meas.*, vol. 31, no. 11, pp. 1467–1485, Nov. 2010.
- [17] B.-U. Köhler, C. Hennig, and R. Orglmeister, "The principles of software QRS detection," *IEEE Eng. Med. Biol. Mag.*, vol. 21, no. 1, pp. 42–57, Jan./Feb. 2002.
- [18] *Medical Electrical Equipment—Part 2-47: Particular Requirements for the Basic Safety and Essential Performance of Ambulatory Electrocardiographic Systems*, International Electrotechnical Commission, IEC Standard 60601-2-47:2012, 2012.
- [19] G. B. Moody and R. G. Mark, "The impact of the MIT-BIH arrhythmia database," *IEEE Eng. Med. Biol. Mag.*, vol. 20, no. 3, pp. 45–50, May/Jun. 2001.
- [20] A. Taddei *et al.*, "The European ST-T database: Standard for evaluating systems for the analysis of ST-T changes in ambulatory electrocardiography," *Eur. Heart J.*, vol. 13, no. 9, pp. 1164–1172, Sep. 1992.
- [21] A. L. Goldberger *et al.*, "PhysioBank, PhysioToolkit, and PhysioNet: Components of a new research resource for complex physiologic signals," *Circulation*, vol. 101, no. 23, pp. e215–e220, Jun. 2000.
- [22] *Testing and Reporting Performance Results of Cardiac Rhythm and ST-Segment Measurement Algorithms*, Association for the Advancement of Medical Instrumentation, AAMI Standard ANSI/AAMI EC57:1998(R)2003, 2003.



DORTHE B. SAADI received the M.Sc. degree in biomedical engineering from the Technical University of Denmark and the University of Copenhagen, Denmark, in 2011. She is currently pursuing the Ph.D. degree with the Department of Electrical Engineering, Technical University of Denmark. Her Ph.D. project is carried out in a close corporation with DELTA and Svendborg Hospital. Her research interests include automatic biomedical signal processing, heart arrhythmias, algorithm design, and clinical validations.



GEORGE TANEV received the B.Eng. degree in biomedical engineering from Carleton University, Ottawa, Canada, in 2008, and the M.Sc. degree in biomedical engineering from the Technical University of Denmark and the University of Copenhagen, Denmark, in 2014. His master's thesis was based on developing a measurement methodology for noninvasive blood pressure. His master's thesis was carried out in close collaboration with DELTA. His research interests include biomedical signal processing, heart rate variability, pulse transit time, portable medical technologies, and real-time embedded systems.



MORTEN FLINTRUP received the M.Sc. degree in information technology from the IT University of Copenhagen, Denmark, in 2004. He is currently a Research and Development Engineer and the Software Team Leader with the ePatch Development Team, DELTA Danish Electronics, Light and Acoustics.



ARMIN OSMANAGIC received the Medical degree from the University of Southern Denmark in 2010. He is currently pursuing the Ph.D. degree with the University of Southern Denmark and the Department of Medical Research, Svendborg Hospital, Denmark.



POUL JENNUM received the Medical degree and the D.Med.Sc. degree from the University of Copenhagen, in 1983 and 1998, respectively. He is currently a Chief Consultant Cardiologist and Professor with the Department of Clinical Neurophysiology, Rigshospitalet, University of Copenhagen, Denmark.



KENNETH EGSTRUP received the Medical degree from Aarhus University, Denmark, in 1975. He was a Certified Specialist in cardiology in 1987, and became a Doctor in medical science with the University of Odense, Denmark, in 1990. Since 1995, he has been a Chief Physician with the Department of Medicine, Section of Cardiology, Svendborg Hospital, Odense University Hospital, and a Professor of Cardiology with the University of Southern Denmark, since 2007. He has been a member of the Strategic Regional Research Council in Region Southern Denmark since 2007. He has received several awards for his research work.



JØRGEN L. JEPPESEN received the Medical degree and the Ph.D. degree in medical science from the University of Copenhagen, Denmark, in 1989 and 2004, respectively. He is currently a Consultant Cardiologist and Professor with the Department of Medicine, Glostrup Hospital, University of Copenhagen.



HELLE K. IVERSEN received the Medical degree and the D.Med.Sc. degree from the University of Copenhagen, in 1985 and 2004, respectively. She is currently a Neurologist and the Head of the Stroke Center Rigshospitalet, Glostrup, and a Clinical Research Associated Professor with the University of Copenhagen, Denmark.



KARSTEN HOPPE received the M.Sc. degree in electrical engineering from the Technical University of Denmark, in 1995. He is currently a Research Manager with the ePatch Group, DELTA Danish Electronics, Light and Acoustics. His main interest is ePatch-based medical device design.



HELGE B. D. SORENSEN (M'90) received the M.S.E.E. and Ph.D. degrees in electrical engineering from the Institute of Electronic Systems, Ålborg University, in 1985 and 1992, respectively. He was initially a Research Assistant with Ålborg University. From 1989 to 1993, he was an Assistant Professor with the Institute of Electronic Engineering, Ålborg University. From 1993 to 1995, he was an Associate Professor with the Engineering Academy Denmark. Since 1995, he has been an Associate Professor and the Head of the Biomedical Signal Processing Research Group with the Department of Electrical Engineering, Technical University of Denmark.